Research Article | Vol. 25, No. 13 | 26 Jun 2017 | OPTICS EXPRESS 15028
Optics EXPRESS

ASK-based spatial multiplexing RGB scheme using symbol-dependent self-interference for detection

STEFANO PERGOLONI, ANDREA PETRONI, THAI-CHIEN BUI, GAETANO SCARANO, ROBERTO CUSANI, AND MAURO BIAGI*

Department of Information, Electrical and Telecommunication (DIET) engineering, "Sapienza" University of Rome, Via Eudossiana 18, 00184 *Rome, Italy.*
Mauro.Biagi@uniroma1.it

Abstract: We propose a vsible light communication scheme utilizing red, green and blue light-emitting diodes (LEDs) and three color-tuned photodiodes. Amplitude shift keying modulation is considered, and its effect on light emission in terms of flickering, dimming, and color rendering is discussed. The presence of interference at each photodiode generated by the other two colors is used to improve detection since interference is symbol-dependent. Moreover, the capability of the photodiodes to follow the LEDs speed is considered by analyzing the possibility of equalizing the received signal, and also self-interference mitigation is proposed. The system performance is evaluated both with computer simulations and tests on an Arduino board implementation.

OCIS codes: (060.2605) Free-space optical communication; (060.4080) Modulation.

References and links

1. H. Elgala, R. Mesleh, and H. Haas, "Indoor optical wireless communication: potential and state-of-the-art," IEEE Commun. Mag. **49**(9), 56–62 (2011).
2. Y. Wang, L. Tao, X. Huang, J. Shi and N. Chi, "8-Gb/s RGBY LED-based WDM VLC system employing high-order CAP modulation and hybrid post equalizer," IEEE Photo. J. **7**(6), 1–7 (2015).
3. J. K. Kwon, "Inverse source coding for dimming in visible light communications using NRZ-OOK on reliable links," IEEE Photon. Technol. Lett. **22**(19), 1455–1457 (2010).
4. K. I. Ahn and J. K. Kwon, "Capacity analysis of M-PAM inverse source coding in visible light communications," J. Lightwave Technol. **30**(10), 1399–1404 (2012).
5. J.-B. Wang, Q.-S. Hu, J. Wang, M. Chen and J.-Y. Wang, "Tight bounds on channel capacity for dimmable visible light communications", J. Lightwave Technol. **31**(13), 37715–3779 (2013).
6. C. H. Yeh, Y. F. Liu, C. W. Chow, Y. Liu, P. Y. Huang and H. K. Tsang, "Investigation of 4-ASK modulation with digital filtering to increase 20 times of direct modulation speed of white-light LED visible light communication system," Opt. Express **20**(15), 16218–16223 (2012).
7. N. Bamiedakis, X. Li, J. J. D. McKendry, E. Xie, R. Ferreira, E. Gu, M. D. Dawson, R. V. Penty and I. H. White, "Micro-LED-based guided-wave optical links for visible light communications", in *Proceedings of IEEE Conference on Transparent Optical Networks* (IEEE, 2015), pp. 1–4.
8. G. Cossu, A. M. Khalid, P. Choudhury, R. Corsini and E. Ciaramella, "3.4 Gbit/s visible optical wireless transmission based on RGB LED," Opt. Express **20**(26), B501–B506 (2012).
9. F. M. Wu, C. T. Lin, C. C. Wei, C. W. Chen, Z. Y. Chen and K. Huang, "3.22-Gb/s WDM visible light communication of a single RGB LED employing carrier-less amplitude and phase modulation," in *Optical Fiber Communication Conference/National Fiber Optic Engineers Conference*, OSA Technical Digest (Optical Society of America, 2013), paper OTh1G.4.
10. Y. Wang, X. Huang, J. Zhang, Y. Wang and N. Chi, "Enhanced performance of visible light communication employing 512-QAM N-SC-FDE and DD-LMS," Opt. Express **22**(13), 15328–15334 (2014).
11. L. Cui, Y. Tang, H. Jia, J. Luo and B. Gnade, "Analysis of the multichannel WDM-VLC communication system," J. Lightwave Technol. **34**(24), 5627–5634 (2016).
12. C. M. Panazio and J. M. T. Romano, "On the convergence of a new joint DFE & decoding procedure for blind decision directed LMS equalization," in *Proceedings of IEEE International Conference on Communications* (IEEE, 2002), pp. 129-133.
13. G. Cossu, W. Ali, R. Corsini, and E. Ciaramella, "Gigabit-class optical wireless communication system at indoor distances (1.5 – 4 m)," Opt. Express **23**(12), 15700–15705 (2015).
14. Y. Wang, L. Tao, X. Huang, J. Shi and N. Chi, "Enhanced performance of a high-speed WDM CAP64 VLC system employing volterra series-based nonlinear equalizer," IEEE Photo. J. **7**(3), 1–7 (2015).

#292707 https://doi.org/10.1364/OE.25.015028
Journal © 2017 Received 13 Apr 2017; revised 13 May 2017; accepted 14 May 2017; published 21 Jun 2017

Optics EXPRESS

15. A. K Jain, "*Fundamentals of Digital Image Processing*," (Prentice-Hall, Inc., 1989), Chap. 3.
16. Z. Wang, W. D. Zhong, C. Yu, J. Chen, S. Francois and W. Chen, "Performance of dimming control scheme in visible light communication system," Opt. Express **20**(17), 18861–18868 (2012).
17. S. Pergoloni, M. Biagi, S. Rinauro, S. Colonnese, R. Cusani and G. Scarano, "Merging color shift keying and complementary pulse position modulation for visible light illumination and communication," J. Lightwave Technol. **33**(1), 192–200 (2015).
18. ITU-T, "Vocabulary for Performance and Quality of Service" (*ITU-T Recom. Part .10* 2006).
19. S. Dimitrov and H. Haas, "*Principles of LED Light Communications: Towards Networked Li-Fi*," (Cambdrige University Ppress, 2015).
20. OSRAM, "*LEDs, New Light Sources for Display Backlighting Application Note*," (OSRAM TLT, 2015).
21. J. R. Barry, J. M. Kahn, W. J. Krause, E. A. Lee and D. G. Messerschmitt, "Simulation of multipath impulse response for indoor wireless optical channels," IEEE J. Sel. Areas Commun. **11**(3), 367–379 (1993).
22. S. R. Perez, R. P. Jimenez, O. B. G. Hernandez, R. Borges, and R. Mendoza, "Concentrator and lens models for calculating the impulse response on IR-wireless indoor channels using a ray-tracing algorithm," Microw. Opt. Technol. Lett. **36**(4), 262–267 (2003).
23. Luxeon Star LEDs, "*Rebel LEDs datasheet*," (Luxeon Star LEDs, 2016).
24. M. Rahaim, T. Borogovac and J. B. Carruthers, "CandLES: Communications and Lighting Emulation Software," in *Proceedings of the fifth ACM international workshop on Wireless network testbeds, experimental evaluation and characterization* (ACM, 2010), pp. 9–14.

1. Introduction

Visible light communications (VLC) can be an effective complementary technology to radio frequency (RF) especially for its flexibility of adoption in places like airplanes and hospitals where the use of RF is limited or forbidden.

Light emitting diodes (LEDs) are increasingly used as a more power efficient illumination sources than incandescent lamps, meeting the requirements for global electromagnetic pollution reduction. Moreover, since LEDs can quick react to driver signals, they allow the accomplishment of data transmission while illuminating which is the distinctive characteristic of a VLC system [1].

This paradigm, *transmitting while illuminating*, adds new constraints to the communication system that are tailored to common lighting standards. In this regard, the problem of dimming has been tackled [3, 4] and inverse source coding is employed for improving the performance of a VLC system working according to non-return-to-zero on-off keying (NRZ-OOK) and M-ary pulse amplitude modulation (M-PAM), respectively. More, since analog dimming reflects on the symbols amplitude change, an optimization method for PAM schemes, based on the probability distribution and intensity of the constellation points, in order to meet the dimming requirements has been proposed in the literature [5].

Still regarding amplitude modulation 4-amplitude shift keying (ASK) modulation and digital filtering are used to enhance the transmission rate of white-light LED in VLC transmission [6]. By employing a commercial LED with a bandwidth of 1 MHz and implementing the receiver with a finite impulse response (FIR) digital equalizer it has been possible to achieve a communication rate of 20 Mbit/s, without using any optical blue filter.

An additional resource for rate improvement is represented by the use of multiple-input multiple-output (MIMO) architectures, in fact, it is known that good performance cannot be achieved using single-input single-output (SISO) solutions [7]. The most significant rate improvement relies therefore on the use of multiple transmitters and receivers with the possibility of following a ganging approach, where all LEDs carry the same data, or a MIMO one where each LED transmits an independent data stream. Furthermore, using red-green-blue (RGB) LEDs is preferable with respect to phospor-based LEDs since each color component has a higher bandwidth and the three different channels can be used for increasing the data throughput. It is important to note that luminaries mainly used for VLC are either phosphor based or three-chromatic LEDs, i.e. RGB LEDs. The former ones are easier to design and less expensive than RGB LEDs, though, due to problems related to the degradation of the phosphor, the

Optics EXPRESS

coating of a blue LED with a yellow phosphor causes a lower luminous efficacy compared with RGB LEDs. More, phosphor-based LEDs have a very limited modulation bandwidth (few MHz). Three-chromatic LEDs, instead, have a higher bandwidth per channel and, moreover, can use three channels for increasing the data throughput. Some schemes using RGB are proposed in the literature [8–10]. One solution [8] considers different modulations formats to achieve a very high data rate, of the order of Gb/s, by using a single commercial RGB-White LEDs and three RGB LEDs. At the transmitter perfect channel knowledge is required in order to perform bit-loading. So the experiment considers a preliminary channel measurement and an off-line optimization. This solution requires that when channel changes due to relative angle or distance between transmitter and receiver variations, the channel must be newly measured and optimization rerun and different light intensities arranged. Moreover, this does not necessarily lead to white light emission. In VLC systems employing wavelength division multiplexing (WDM) an important issue is the channel crosstalk due to the presence of spectral overlap over different colors, even when optical filters are applied at the receiver. The impact of this issue on the VLC performance has been recently studied [11]. In this regard, one work [9] measures the effect of interference of other colors on the main color (for example bite error rate (BER) reduction due to green and blue component on a red channel). A pre-compensation filter at the transmitter is adopted as well as a digital feedback equalizer (DFE) at the receiver. DFE so requiring channel knowledge that is assumed present both at the transmitter and the receiver.

In a different and interesting work, least mean square with decision directed mechanism is considered with 3 LEDs and 3 photodiodes [10]. Experimental results report that, using a 512-quadrature amplitude modulation (QAM) scheme, a peak data rate of 4.22 Gb/s has been achieved, although measured at a 1 cm distance and considering a remarkable per channel bandwidth of about 156 MHz. That scheme still assumes to have perfect channel knowledge at the transmitter since pre-equalization is performed and the Authors claims for equalization of channel with 3 to 53 taps. This is very costly for a computational point of view and misconvergence of the equalizer is not discussed [12]. A further data rate improvement is presented later [2] using an additional channel (yellow) and carrierless amplitude phase (CAP) modulation, however the issue of having complex equalization mechanism still hold true.

Some of the above cited contributions present high data rate systems, even though considering a very limited communication distance in the order of few centimeters. In this sense, remarkable improvements are highlighted in the literature where the authors demonstrate a WDM based VLC link able to perform over a range between 1.5 and 4 meters [13]. By using an avalanche photodiode module and a commercial red-green-blue-yellow (RGBY) in a 4-channel transmission implemented with discrete multitone modulation, bit loading and power loading, a maximum aggregate data rate of 5.6 Gbit/s is achieved at 1.5 meters. Still, perfect channel knowledge is assumed and the received data are offline processed. Moreover, lighting constraints are demonstrated to be met, providing also an overall white light emission. Another WDM VLC architecture has been successfully tested over a 2 meters indoor channel [14]. Signal pre-equalization and CAP modulation allow the achievement of a 4.5 Gb/s rate by using commercial RGB LEDs and photodiodes. High performance in terms of BER are guaranteed by a Volterra nonlinear equalizer implemented at receiver side in order to compensate the nonlinear behavior of the LED. By observing what the literature has proposed till now, it appears that the high data rates achieved are mainly due to the large band of the system and rich modulation formats employed. Equalization mechanisms at the receiver are well performing but, sometimes, very costly. Furthermore the perfect channel knowledge at the transmitter, very often assumed, constrains the analysis to a static channel scenario. hence, in the recent past, few attention has been paid to realistic assumptions towards the implementation of a communication system. Moreover, no considerations about the complexity of the processing required to perform detection have been usually carried out. Besides solutions that claim for ability of tracking channel

Optics EXPRESS

performed tests without any mobility.

For the above reasons, we propose a system employing ASK modulation where white light should be granted as a constraint and we employ three LEDs one tuned on red, one on green and one on blue. We measured the quality of light in terms of brightness and color rendering perceived by people via subjective tests. We use also three photodiodes at the receiver each one tuned on the above emitted colors. The choice of using multiple LEDs in place of a single white LED is justified by the possibility of increasing rate by resorting to the MIMO paradigm of spatial multiplexing. The choice of using multiple photodiodes is because this allows to have less costly processing operated in parallel. Moreover, our detection mechanism aims at reducing interference from different colors to the detected one (from example green and blue on red) but, at the same time, it uses interference for detection since it carries information. We provide also an experimental setup based on Arduino-Due board.

2. System model

Let us consider the presence of three LEDs (as depicted in Fig. 1), each tuned on a different wavelength, namely, red, green and blue (RGB), so to have as transmitted signal in the signaling interval T_P

$$s(t) = \sum_{c \in C} A_c s_c(t) \tag{1}$$

where the set $C = \{R, G, B\}$ collects the three different colors, the term $A_c \in \mathcal{A} = \{1, 2, \ldots, M\}$ can assume each of the M different amplitudes and $s_c(t)$ is the signal representing the light emitted by the c-th color LED in a non-return-to-zero (NRZ) way. It is important to note that different colors exhibit different $s_c(t)$. The presence of the term A_c implicitly means that the

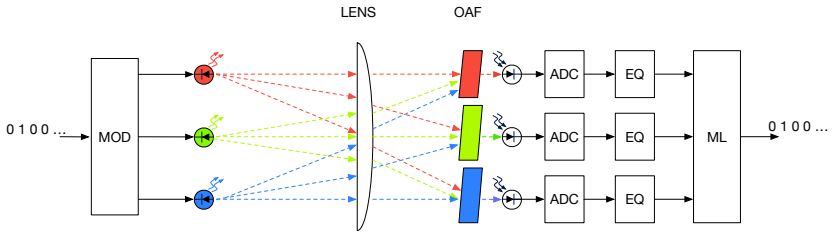

Fig. 1. Scheme of the transmitter, channel and receiver.

R, G, B LEDs can, symbol by symbol and LED by LED, emit different light intensities. Since this reflects also on illumination service, it is important to analyze the relationship with respect to three different issues. The first one is related to the flickering of the light [15] Chap. 3, while the second one deals with dimming [16]. The third aspect is the color rendering [17]. To handle these three light emission aspects we need to resort to the human eye properties and behavior.

Flickering effect, that is, the sensation of changes in light intensity is ruled by the second Bloch's law [15] in Chap.3 which states that the human eye is able to perceive light intensity changes if the flashing frequency is of the order of 50÷ 100 Hz. In our scheme this would

Optics EXPRESS

imply $T_P = 10ms \div 20ms$, and since we do not work with such a high value of signaling time, flickering is totally avoided in our system.

Regarding dimming, we should start by considering the (average) power, measured on a time interval that is the one the retina needs to measure light ($T_{retina} = 20ms$). The number of symbols transmitted by the LEDs within T_{retina} is $N_s = \lfloor T_{retina}/T_P \rfloor$ so the power is measured as:

$$\mathcal{P} = \frac{1}{T_{retina}} \int_{T_{retina}} \sum_{p=1}^{N_s} \sum_{c \in C} A_c(p) s_c(t - pT_P) dt. \tag{2}$$

If we compare this value with the one obtained with a fixed light in the same interval

$$\mathcal{P}^{(ill)} = \frac{1}{T_{retina}} \int_{T_{retina}} \sum_{c \in C} A_c^{(ill)} dt \tag{3}$$

$A_c^{(ill)}$ being the color light intensity used for illumination, we find that the difference is

$$\Delta\mathcal{P} = \mathcal{P}^{(ill)} - \mathcal{P} =$$

$$\frac{1}{T_{retina}} \int_{T_{retina}} \sum_{c \in C} \left(A_c^{(ill)} - \sum_{p=1}^{N_s} A_c(p) s_c(t - pT_P) \right) dt \tag{4}$$

As will be clearer in section 4.2 this difference is not perceived by the human eye as confirmed by the tests based on mean opinion score (MOS) that is a subjective measure of the quality based on the perception of users [18].

About color rendering, we can refer to the color matching theory [15] Chap. 3, and, by resorting to the international commission on illumination (CIE) 1931 diagram, we know that with three primary colors we can have all the possibilities within the triangle whose vertexes are on the boundary of the diagram in correspondence of the primary wavelengths. This is reported in Fig. 2 where the lines connecting the vertexes represent the bound of the colors that can be obtained. This implies that, symbol by symbol, the color obtained with the LEDs is not the same over time. In this context, Fig. 2 represents the colors affordable for an assigned light intensity level and in particular we indicate with two circles the color related to the symbol $(A_G, A_R, A_B) = (4, 4, 4)$ and $\{A_G, A_R, A_B\} = \{4, 2, 1\}$, when M=4.

Also in this case, we can refer to the time needed by retina to acquire a signal in order to evaluate the colors emitted by the LEDs. This can be easily evaluated via short time Fourier Transform. Hence, the spectrum is essentially given by:

$$X(f) = \frac{1}{T_{retina}} \int_{T_{retina}} \sum_{p=1}^{N_s} \sum_{c \in C} A_c(p) s_c(t - pT_P) e^{-i2\pi ft} dt \tag{5}$$

As it is possible to note from (5), different color components are present and the perceived color is expected to be a *mixture* of different levels of white and other colors ranging from red to green and blue. Also in this case, for a fast signaling rate, the second Bloch's law helps our discussion. In fact, when the maximum light level is emitted, a high light intensity (white) is obtained. Other colors, with lower light intensity are essentially not perceived due to the band-pass behavior of the eye with respect to the quick transition (of the order of milliseconds or less) of the light intensity. To corroborate this conjecture, we report in section 4 the evaluation of the perceived color with a MOS test.

Still regarding the system architecture proposed in this work, at the receiver we assume to have 3 different photodiodes each one tuned on the corresponding R, G, B LEDs. This is possible thanks to the use of optical analog filters (OAFs) as depicted in Fig. 1. Hence, the first

Optics EXPRESS

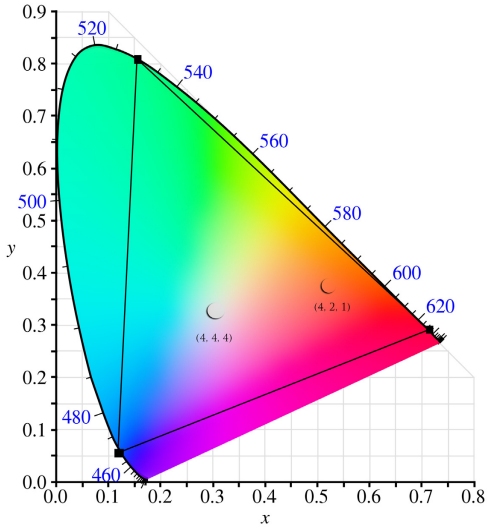

Fig. 2. CIE 1931 diagram with primaries and an example of symbol (4,4,4) and (4,2,1).

photodiode is tuned on red, the second on green and the third one on blue. This can be obtained by using colored transparent stripes. Summarizing, we consider a MIMO architecture with 3 transmit LEDs and 3 receive photodiodes. The channel impulse response between the c-th LED and j-th photodiode is denoted as $h_{cj}(t)$. The composite MIMO channel response is

$$\mathbf{H}(t) = \begin{bmatrix} h_{RR}(t) & h_{RG}(t) & h_{RB}(t) \\ h_{GR}(t) & h_{GG}(t) & h_{GB}(t) \\ h_{BR}(t) & h_{BG}(t) & h_{BB}(t) \end{bmatrix} \tag{6}$$

As an example, the vector $[h_{RR}(t)\ h_{RG}(t)\ h_{RB}(t)]$ is essentially the spatio-temporal signature induced by the red light across the three photodiodes thus meaning that we can measure the pulse emitted by red LED from three different points of view. The matrix structure induces the following remark related to correlation among channels, both from a space and time point of view. With the above matrix, we are in the presence of nine channels. If the channels are spatially correlated, we cannot distinguish among the different components also in the presence of perfect channel knowledge at the receiver. This is essentially due to the impossibility of inverting the effect of channel matrix and process it to obtain a diagonal one. Proper spacing of LEDs can reduce correlation [19] in Chap. 6 and this allows also a better light pointing if needed for illumination purposes [20]. The above formulation allows us to detail the received signal. In fact, given that the signal $A_c s_c(t)$ is emitted by the c-th LED, the whole signal received at the j-th photodiode (with $j \in C$) is given by

$$y_j(t) = \sum_{c \in C} A_c s_c(t) * h_{cj}(t) + w_j(t) \tag{7}$$

where $*$ is the convolution operator, $h_{cj}(t)$ is the whole channel impulse response, that is generic element of the matrix $\mathbf{H}(t)$, while $w_j(t)$ is the additive white Gaussian noise. Before proceeding, it is mandatory to explain the role played by $h_{cj}(t)$ and the different features that compose the channel impulse response. The term $h_{cj}(t)$ can be exploded as follows

$$h_{cj}(t) = f_L(t) * f_{cj}(t) * f_{PD}(t) * f_{FSP_{cj}}(t) \tag{8}$$

Optics EXPRESS

where $f_L(t)$ models the effect of a possibly present lens used to focus the light beam as depicted in Fig. 1 and its modeling can be easily obtained [22]. Furthermore, $f_{cj}(t)$ in (8) is the impulse response of the OAF represented by the above mentioned colored transparent stripes tuned on LEDs. Moreover $f_{PD}(t)$ in (8) is the channel impulse response of the photodiode. Last, $f_{FSP_{cj}}(t)$ is the effect of free space propagation from the LED associated to the c-th color to the j-th photodiode that can be modeled according to geometrical parameters. About free space propagation [21], we consider $f_{FSP_{cj}}(t)$ without reflectors. In the more general case with the presence of reflectors, the channel will be wavelength-selective [21]. The referred model considers also the effect of the wavelength. So the propagation follow the following rule:

$$f_{FSP_{cj}}(t) \approxeq \frac{m+1}{2\pi} \cos^m(\phi) d\Omega \, \mathrm{rect}(\theta/FOV) \delta\left(t - d_{c,j}/v\right), \tag{9}$$

where FOV is the field of view angle and $d\Omega$ is the solid angle subtended by the receiver differential area, by assuming A_e (detector size) $<< d_{c,j}^2$, with d distance between the transmitter and receiver and v the propagation speed,

$$d\Omega = \cos(\theta) A_e / d_{c,j}^2, \tag{10}$$

while ϕ is the angle of irradiance, θ is the angle of incidence with respect to the receiver axis, and m is Lambertian order that characterizes the light beam directivity. In this regard, it is possible to consider the amplitude of the received signal as:

$$a(d) = \frac{m+1}{2\pi} \cos^m(\phi) d\Omega \, \mathrm{rect}(\theta/FOV). \tag{11}$$

Still about the mathematical properties of the channel, we highlight that the ideal case for RGB components is $h_{cj}(t) = 0, c \neq j$ thus meaning that, for example, the red component is not received by the G and B tuned photodiodes so the interference between colors (named self-interference) is absent, thus meaning that the matrix $\mathbf{H}(t)$ is diagonal. However, this is not true in general and self-interference is expected to be present at the photodiode. This kind of interference is essentially among spatial symbols, that is, spatial intersymbol interference (ISI). Still about non-idealities, it is also possible that the $f_{PD}(t)$ term is not able to *follow* the dynamic behavior of LED so introducing time dispersion, that is, temporal ISI.

3. Detection mechanism

Before detailing the detection mechanism, it is fundamental to consider one key point. In this system the interference generated by the color cross talk has a twofold nature. From one hand interference is an impairment for the reliability of the communication link, while from the other side interference carries information since it is tied to the symbol emitted by other LEDs (*other* with respect to the color-tuned photodiode). While it is not difficult to explain why interference can be disruptive for a communication, it is not so intuitive to explain why it can be useful. The detection of the symbol related to the c color on the $j = c$ photodiode depends on the received signal that is the sum of the effect of the channels on the symbols emitted by all the LEDs so leading to have the symbol-dependent interference as reported in (7). Hence, the idea for performing detection is to take into account not only the symbols that the c-th LED can emit but also all the possible symbols emitted by the other (two) LEDs, filtered by the channels. Moreover, we perform joint detection (and not separated on the three branches), that means, having a joint measure of useful signal and interfering ones since the signal emitted by a LED has three different versions at the photodiodes. The detailed description of the mechanism will specify this latter argumentation.

The preliminary action to take into account is the transmission of a pulse by each LED (with the other LEDs turned off) so giving rise to a training sequence. This corresponds to assume

Optics EXPRESS

that the transmitted matrix, that collects in the rows the symbols transmitted by the 3 LEDs, is the identity one. In this way, for example, when the red pulse is sent, the signal at the j-th photodiode will be

$$y_j(t) = A_R s_R(t) * h_{Rj}(t) + w_j(t) \tag{12}$$

and, since both the training amplitude A_R and signal $s_R(t)$ are known to the j-th receiver, this latter can estimate the channel impulse response. Since we will deal with discrete time estimation, we need to preliminary sample the received signal $y_j(t)$ so to have $y_j(nT_s)$, T_s being the sample time. This operation is performed by the analog to digital converter (ADC) as depicted in Fig. 1. In this way, by extending this mechanism to all the RGB components, we can observe that the estimation $\tilde{h}_{cj}(nT_s)$ of the discrete time channel $h_{cj}(nT_s)$ can be obtained thanks to the training operation.

A simple way of proceeding is to work in the frequency domain since we deal with energy components so, by considering $H_{cj}(k)$ as the discrete Fourier transform (DFT) of $h_{cj}(nT_s)$, we have that the estimation $\tilde{H}_{cj}(k)$ is given by

$$\tilde{H}_{cj}(k) = \frac{Y_j(k)}{S_c(k)} \tag{13}$$

where $Y_j(k)$ is the DFT of $y_j(nT_s)$ and $S_c(k)$ is the DFT of the sampled pulse transmitted by the c-th color $s_c(nT_s)$. The discrete time version of the estimation can be obtained by applying the inverse DFT to $\tilde{H}_{cj}(k)$. The next step is related to the detection of data symbols. At the j-th branch, corresponding to the j-th photodiode chain, a ($N_P \times M^2$ matrix) named $\mathbf{Z}_j$ is built and it is defined as follows

$$\mathbf{Z}_j = [\mathbf{z}_j^{(A_{c_m}=1, A_{c_l}=1)} \ldots \mathbf{z}_j^{(A_{c_m}=M, A_{c_l}=M)}] \tag{14}$$

that is the collection of the column vectors $\mathbf{z}_j^{(A_{c_m}=m, A_{c_l}=l)}$ each one gathering N_P samples, where $N_P = \lfloor T_P/T_s \rfloor$. The generic element of the matrix $\mathbf{Z}_j$ is given by

$$\mathbf{Z}_j[n, v] = y_j(nT_s) - \sum_{c_v \in C/\{j\}} A_{c_v} s_{c_v}(nT_s) * \tilde{h}_{c_v j}(nT_s). \tag{15}$$

that is the received sample where we subtract the value of interference by exploring all the M^2 values for the symbol emitted A_{c_l} and A_{c_m}. It is worth noting that the term v is an auxiliary variable we use to span the M^2 values and it is formally defined as $v = (m-1)M + l$ where m and l are the m-th and l-th symbols emitted by c_m-th and c_l-th interfering LEDs respectively, while c_v collects the pair of colors c_m and c_l. Hence the use of v helps to sort in the matrix $\mathbf{Z}_j$ the symbols emitted by the interfering LEDs.

As previously disclosed, it is possible that the j-th photodiode is unable to present raise and fall times comparable with LEDs speed, hence an equalization, operated on the sampled signal, must take place. A possible implementation is the zero forcing (ZF) one, which consists in estimating the channel between the reference LEDs and the tuned photodiode $\tilde{H}_{jj}(k)$ obtaining its reciprocal $G_{jj}(k) = \tilde{H}_{jj}^{-1}(k)$ and then inverting it according to the inverse DFT, so as to arrive at $g_{jj}(nT_s)$. This allows to consider the equalization as the convolution between each of the columns of $\mathbf{Z}_j$ and $g_{jj}(nT_s)$. So, the output of the convolution can be organized in the ($N_L \times M^2$) matrix $\mathbf{X}_j$ defined as follows

$$\mathbf{X}_j = [\mathbf{x}_j^{(A_{c_m}=1, A_{c_l}=1)} \ldots \mathbf{x}_j^{(A_{c_m}=M, A_{c_l}=M)}] \tag{16}$$

where $N_L = N_P + N_{eq} - 1$ is the number of samples of the equalized sequence by considering also the equalizer length N_{eq}, and the general vector $\mathbf{x}_j^{(A_{c_m}=m, A_{c_l}=l)}$ is the output of the convolution

$$\mathbf{x}_j^{(A_{c_m}=m, A_{c_l}=l)} = \mathbf{z}_j^{(A_{c_m}=m, A_{c_l}=l)} * g_{jj}(nT_s). \tag{17}$$

Optics EXPRESS

Before proceeding two elements must be highlighted. First, the value assumed by $\mathbf{x}_j^{(A_{cm}=m, A_{cl}=l)}$ is influenced by several terms. In fact, by observing (7), (15) and (17) one can argue that $\mathbf{x}_j^{(A_{cm}=m, A_{cl}=l)}$ collects the samples of data emitted by the c-th LED, filtered by the channel $h_{cj}(t)$ and equalized with $g_{jj}(nT_s)$. Second, it contains also residual self-interference, filtered by the channels $h_{cmj}(t)$ and $h_{clj}(t)$ and the above reported equalizer and, more, noise samples that are no more temporally white since colored by the equalizer. Since we are interested in measuring what happens every signaling time, we can sum over N_L samples, in order to obtain the energy of the signal, this corresponds to sum the elements of the matrix $\mathbf{X}_j$ on each column so as to obtain a single $(1 \times M^2)$ row vector

$$\mathbf{q}_j = \sum_{n=0}^{N_L-1} \mathbf{X}_j[n, v] \tag{18}$$

whose generic element $\mathbf{q}_j[v]$ is

$$\mathbf{q}_j[v] = \sum_{n=0}^{N_L-1} \mathbf{x}_j^{(A_{ck}=k, A_{cl}=l)}. \tag{19}$$

In order to show how different elements of the transmission/reception chain impacts on term $\mathbf{q}_j[v]$, we expand it so as to show the dependencies

$$\begin{aligned}\mathbf{q}_j[v] = &\sum_{n=0}^{N_L-1} \left[\sum_{c \in C} A_c s_c(nT_s) * h_{cj}(nT_s) * g_{jj}(nT_s) \right] - \\ &\sum_{n=0}^{N_L-1} \left[\sum_{c_v \in C/\{j\}} A_v s_{c_v}(nT_s) * \tilde{h}_{c_v j}(nT_s) * g_{jj}(nT_s) \right] \\ &+ \sum_{n=0}^{N_L-1} w_j(nT_s) * g_{jj}(nT_s).\end{aligned} \tag{20}$$

In order to perform detection, we gather in the $(1 \times M)$ row vector $\mathbf{u}_j$ the useful signal at the j-th photodiode when all possible M symbol emitted by the c-th LED (with $c = j$) are considered. So, by assuming to indicate as $p = 1, \ldots, M$ the index of the ASK symbol emitted by the c-th LED ($c = j$), the generic element of $\mathbf{u}_j$ is

$$\mathbf{u}_j[p] = \sum_{n=0}^{N_L-1} A_j[p] s_j(nT_s) * h_{jj}(nT_s) * g_{jj}(nT_s). \tag{21}$$

This allows us to evaluate the *distance* between two terms. The first one is the received sequence when interference subtraction is considered by accounting for all possible transmitted symbols, while the second one is the filtered version of useful signal as in (21). This distance, measured at the j-th photodiode depends on the symbol (p) emitted by the j-th LED (with $j = c$) and the possible interference symbols (v) belonging to other colors:

$$\delta_{j,p,v} = (\mathbf{q}_j[v] - \mathbf{u}_j[p])^2. \tag{22}$$

By considering the three different branches, we can have a joint measure $\Delta_{p,v}$ defined as

$$\Delta_{p,v} = \sum_{j=1}^{3} \delta_{j,p,v}. \tag{23}$$

Optics EXPRESS

Table 1. Model Parameters

LED transmitters	
red wavelength	627 nm
green wavelength	530 nm
blue wavelength	470 nm
maximum transmit power	1.1 W
modulation bandwidth	120 MHz
beam angle	125° FWHM (full width half maximum)
lens	30°
receiver Telstore C7718	
FOV	65°
wavelength range	400 nm - 700 nm
maximum sensitivity wavelength	500 nm
area	1.75 mm^2
effective area A_e	5 mm^2
receiver Vishay BPW34	
FOV	65°
wavelength range	430 nm - 1000 nm
maximum sensitivity wavelength	850 nm
area	0.78 mm^2
effective area A_e	3.3 mm^2

Now, since noise is Gaussian and that its components are spatially uncorrelated, the maximum likelihood criterion asking for maximizing the conditional probability can be solved according to the following criterion

$$\{\hat{A}_R, \hat{A}_G, \hat{A}_B\} = \underset{A_R, A_B, A_G}{\operatorname{argmin}} \Delta_{p,v}, \tag{24}$$

by recalling that the indexes p and v in (23) contain p, l and m. Furthermore, when j is the red photodiode, l and m refer to the symbol emitted by green and blue respectively, when j is the green photodiode, l and m refer to the symbol emitted by red and blue respectively, while if j is the blue photodiode, l and m refer to the symbol emitted by red and green respectively.

Remark - about optimality and complexity

To solve the issues of interference mitigation and channel equalization, the proposed scheme is not the optimal one since the optimal solution requires to have a 3×3 set of Wiener filters in order to equalize both the direct channel, for example $h_{RR}(t)$ and the interfering ones. However, the use of OAF filters allows the receiver to work with signals (on each branch) in the presence of reasonable signal to interference ratio. Moreover, as already specified, this solution with respect to the optimal one is less costly since it has 3 filters in place of 9. Furthermore, even though the use of 3 equalization filters may appear more complex with respect to a single equalizer operating on the three components, we can argue that the channels are shorter if compared with the whole channel (RGB to a single photodiode) so reducing the complexity of each equalizer. Finally, the cost in the detection phase is M^3 since this latter is the number of elements to consider in (24).

4. Numerical results and implementation

We evaluate the performance of the scheme here presented both with Matlab simulations and implementation of a small testbed based on Arduino boards. In the simulations we use the modeling as for the elements we use in the implementation as, for example, LEDs and photodiodes.

Optics EXPRESS

4.1. Numerical results

For what concerns performance comparison we refer to the work where a 4-ASK modulation is used [6]. We recall that white-light is used in that MIMO scheme, while RGB LEDs are considered for our system. For what concerns LEDs, we refer to the Luxeon Star Rebel Red, Green and Blue [23]. We summarize the key elements in Table 1. Furthermore we suppose to drive signal generation with a square root raised cosine signal [6] with signalling period T_P equating 100ns. Hence, for the sake of fairness, in this set of simulations we used a modulation bandwidth of 10MHz. This assumption leads to have for our system three times the rate of the MIMO white

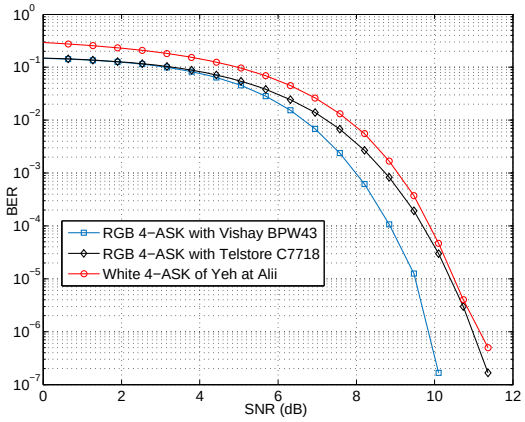

Fig. 3. BER comparison between the proposed scheme with Vishay BPW34 and Telstore C7718 photodiodes and MIMO white LEDs [6].

LEDs [6] when we use 4-ASK, that is 60Mb/s since we use three LEDs in place of one, while MIMO with white LEDs achieves 20Mb/s. The channel is simulated by using MATLAB based CandLES tool [24]. While the FIR filter proposed for MIMO white LEDS [6] has 13-taps length and a particular setup is performed in order to guarantee convergence, no special setup is needed in our scheme and the periodical (i.e. every 2000 symbols) re-estimation is performed without memory, that is, from scratch. In Fig. 3 we reported the BER by considering different signal-to-noise ratio (SNR) levels and we show that the proposed RGB-ASK system achieves lower BER values. In particular using a Vishay BPW34 photodiode leads to obtain better performance with respect to use Telstore C7718 since the equalizer is shorter and more reliable so equalization performs better. The gain offered by the proposed scheme can be justified by observing that the presence of self-interference can help the detection since it is based on the knowledge of possible amplitudes associated to the other color components.

Some schemes proposed in the literature are able to achieve higher rates. This is essentially due to two aspects. First, the bandwidth used is higher, thus meaning, higher symbol rate. Moreover, high-order constellations are used at close distance and the performance falls short when distance increases. In order to measure the performance of the proposed system with respect to the symbol rate (thus meaning the bandwidth of the driving signal), we report in Fig. 4 the achieved BER when 2-ASK, 4-ASK and 8-ASK are used. The considered symbol rate on each branch is on the horizontal axis. It is important to highlight that we perform simulations under the hypothesis of using the same modulation bandwidth on each branch [10], hence the rate is the same for each color. This leads to consider modulation bandwidth levels ranging from 10MHz till to 250MHz and the value on the horizontal axis, in Msymbols/s is *numerically* equivalent to the bandwidth. Basing on that, the transmitted rate is given by the product of sym-

Optics EXPRESS

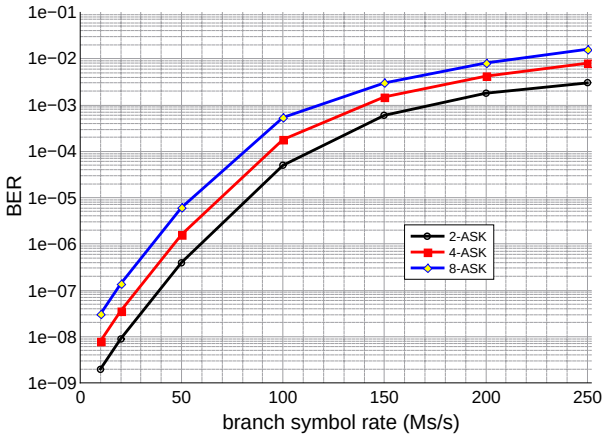

Fig. 4. BER for different values of symbol rates on each transmitting branch and modulation order.

bol rate and the term $3\log_2 M$ where M is the modulation order, so when 10Ms/s is considered for each LED (10MHz), we range from 30Mb/s of 2-ASK to 90Mb/s of 8-ASK. On the extreme right side, a symbol rate of 250Mb/s (that is 250MHz per LED) deals to a rate of 750Mb/s for 2-ASK till to 2.25Gb/s for 8-ASK. The computer simulations refer to a distance of 80cm while for increasing the symbol rate we reduce the signaling time. Figure 4 shows that for relatively low rates (values below 50Ms/s, hence 50MHz per LED, leading to rates ranging from 150Mb/s to 450Mb/s) the BER is below 10^{-5} while it increases when we consider higher rates. The BER obtained at 250MHz is poor and the reason is that the equalizer is unable to consider the limits given by photodiode bandwidth, channel and LED modulation bandwidth. We remark that no coding is present here thus meaning that, in example, the error rate can be reduced with a coding scheme as block coding even though at the expense of reducing information rate, that is, net rate.

4.2. *Implementation*

In Fig. 5 we report a picture of the implemented system that reflects the scheme reported in Fig. 1 when the transmitter and receiver have 30 cm distance for sake of picture representation. It is possible to recognize the Arduino board for signal modulation connected to the LEDs that are red, green and blue whose features are reported in Table 1. LEDs are spaced 2.5cm each other and able to emit an illumination level of 336 lumen. Moreover, lenses with an angle concentration of 30° are used. Furthermore the OAFs are disposed in front of each photodiode (spaced-apart of 2.5cm, Telstore C7718 are used in the picture) and the Arduino (receiving) board processed the received signal. We drive the emission via a Arduino-Due signal generator and control board. Also the receiver is reported and it is possible to recognize that the photodiodes have an OAF each tuned on a different color. The three lenses are posed at 3cm from each LEDs and in the reported results we pose the receiver 97cm from the transmitter if not differently specified. We proper manage Arduino-Due *sketch* in order to manage a maximum aggregate symbol rate till to 84Mb/s by resorting to its clock read status (it has 84MHz processor). The signal is acquired with a Arduino-Due board sampled with 10 quantization bits via the USB/serial port. The data are then visualized and saved on a dialog windows controlling the serial port. After all the data are imported on Matlab where operations like, channel estimation, channel equalization and data detection are performed according to the mechanisms previously

Optics EXPRESS

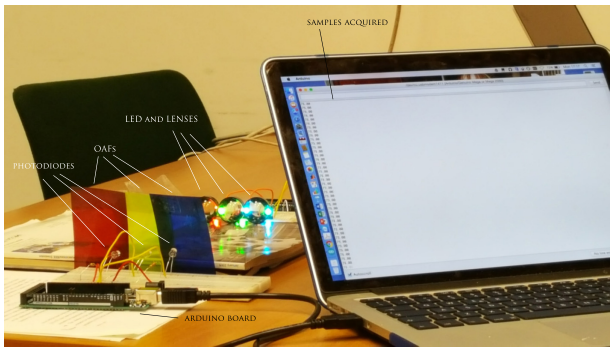

Fig. 5. Picture of the implementation of the system. On right hand side transmitter, on left side receiver with AOFs.

detailed.

In order to both test the performance in terms of BER and check the validity of simulations in the previous subsection, we report in Fig. 6, the BER as a function of distance between transmitter and receiver, when Vishay BPW34 photodiodes are used for 2-ASK, 4-ASK and 8-ASK. We detail the performance for test and simulations. The illumination level is the same while the rate is different. In fact, for 2-ASK we achieve 28Mb/s, for 4-ASK 56Mb/s and 8-ASK 84Mb/s (with a modulation bandwidth of the driving signal of 9.3MHz). It is possible to appreciate that the difference between the implementation results (continuous lines) and simulated ones (dash lines) is really limited. As expected, 8-ASK performs worse with respect to 4-ASK and 2-ASK even though 8-ASK achieves higher bit rate. We remark that at 1 meter the performance for 2-ASK and 4-ASK are around/below a BER of 10^{-3}. In Fig. 7, we discuss the role played

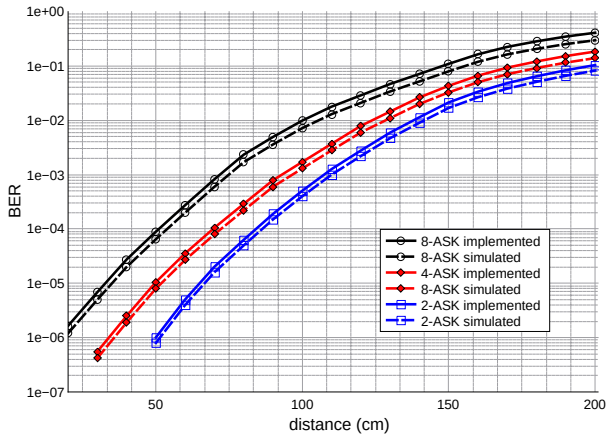

Fig. 6. BER evaluation as a function of distance.

by training. We detail the BER achieved when the frequency of training symbols decreases. Having a low training frequency means that the receiver is not updated about possible channel changes, while a frequent training signaling allows the receiver to be updated at the cost of lowering the net transmission rate. In order to test the behavior of the system when channel changes we slightly move the receiver with respect to its initial position that is 40 cm, 10 cm ahead and

Optics EXPRESS

10 cm back on a small carriage at a speed of approximately 5cm/s so as to induce changes in the channel and test the behavior of the system. In this case we compare the use of Vishay BPW34 and Telstore C7718 photodiodes for 2, 4 and 8-ASK. It is possible to appreciate in Fig. 7 the BER as a function of much frequent estimation is performed. So, a value of ten means that training symbols are sent every 10 data symbols (and this reduces the data rate of 9%). In Fig. 7, all the configurations, that is, photodiodes used and modulation formats, present constant BER values till to the case of training symbols sent every 1000 data symbols (rate reduction 0.1%). When we consider the case of 10000 symbols sent without any training the BER increases till to achieve values of the order of $10^{-7} \div 10^{-6}$. When the training becomes more sporadic the performance falls short since the BER achieves values around $10^{-2} \div 10^{-5}$. From this, we can conclude that sending training every 1000 symbols is a very good compromise when the movement of the receiver is in line with the above described behavior. Vishay photodiodes performs better since the equalizer is shorter (in terms of number of samples) with respect to that required by Telstore one, since the former is able to *follow* the symbol rate. However its gain with respect to a less performing photodiode is limited. Higher BER values achived for sporadic signaling are due to the outdated version of the channel available at the receiver since it uses for detection mechanism an *old knowledge* about the channel and, by considering that changes in distance and angle incurs, the variations can be sensible.

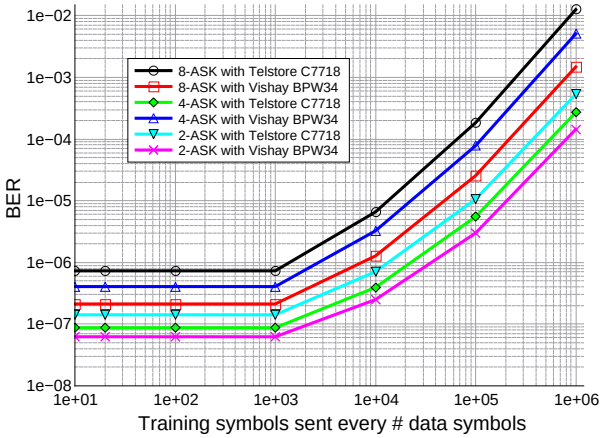

Fig. 7. BER evaluation as a function of training sequence frequency when the receier is moving.

4.3. *Illumination issues: subjective tests*

About color rendering, we asked 50 candidates with age ranging from 22 to 60 years old to evaluate the quality of the white (light) we obtain with the three LEDs. We projected the light constituted by the above mentioned RGB LEDs on a white paper and the candidates were asked to evaluate the white quality by classifying it in white, white with some red components, white with green components, white with blue components and white with other components (oc) that means yellow, magenta and cyan. The result of the mean opinion score is reported in Table 2. It is possible to note that 48 out 50, that is 96%, recognize the light as pure white, independently of the number of symbols constituting the modulation constellation. On the other hand, 1 out of 50, that is 2% recognizes the light as white with some elements of green, while 1 has the perception of a white/red light with 2-ASK and 4-ASK. For 8-ASK one has the perception of white/blue light and one white/red. These results allow us to conclude that the human eye is

Optics EXPRESS

very low sensible to the use of different symbols when ASK is used, so the color rendering is really good.

Table 2. Mean Opinion Score on color rendering on 50 candidates

modulation	white	white/red	white/green	white/blue	white oc
2-ASK	48	1	1	0	0
4-ASK	48	1	1	0	0
8-ASK	48	1	0	1	0

Table 3. Mean Opinion Score on light intensity on 50 candidates

modulation	bad	poor	fair	good	excellent
2-ASK	0	0	0	1	49
4-ASK	0	0	0	1	49
8-ASK	0	0	0	1	49

The same kind of test has been executed with the same sample regarding the level of illumination by using as reference all the lights always on with a $A_c^{(ill)}$ that corresponds to the maximum light intensity of the ASK modulation signal. The results are reported in Table 3. We asked the 50 candidates to give a score from 1 (bad) to 5 (excellent) with possible choice of 2 (poor), 3 (fair), 4 (good). The sample experienced a light illumination level that is for the 98% equal the the one used for illumination when the maximum level is held constant. More, also in this case, the ASK modulation format does not influence the evaluation in the sense that the light intensity is perceived as the same for 2, 4, 8 ASK.

5. Conclusion

We proposed a VLC scheme using ASK characterized by three LEDs, red green and blue, and three photodiodes each tuned on the three components respectively. We detailed a mechanism that implicitly uses the effect of self-interference since this latter is symbol-dependent. Furthermore, we numerically evaluated the performance and compared it with another scheme from the literature. Moreover, we implemented the scheme on a Arduino board and presented the test results. We obtain a good illumination level and color rendering as underlined by subjective measurements. Furthermore, dealing with communication aspects, we perform better with respect to a MIMO scheme operating with white LEDs proposed in the literature and our scheme is a good candidate for real-time implementation since it presents low complexity and does not assume perfect knowledge about channel. Further developments will deal with implementation at higher speed with respect to the maximum shown in this contribution.